

# A Path Following Control of an Unmanned Autonomous Forklift

Tua Agustinus Tamba, Bonghee Hong, and Keum-Shik Hong\*

**Abstract:** In this paper, the development of an unmanned autonomous forklift is discussed. A system configuration using vision, laser ranger finder, sonar, etc. for autonomous navigation is presented. The kinematics of a spin-turn mechanism is analyzed first, and then the obtained kinematics equations are transformed to the equations represented by path variables. These equations are nonlinear state equations to be used for control purposes. A time varying feedback control law via the chained form of Murray and Sastry [12] is derived. The effectiveness of the proposed control law is examined through simulations and experiments.

**Keywords:** Chained form, feedback control, kinematics, path variables, unmanned forklift.

## 1. INTRODUCTION

The demand toward a higher level of automation has changed the way that today's warehouses and distribution centers operate. An ordinary industrial (or warehouse) human-operated forklift needs to be improved to achieve an efficient automated industrial task in the material handling process, while at the same time its operational safety must be assured. With the rapid advances in sensor and computer technologies, the opportunities for developing an autonomous forklift are immense. This paper discusses a system configuration and a path following control algorithm for the development of an unmanned autonomous forklift.

In recent years, there have been an increasing number of researches on the subject of unmanned vehicle navigation. Examples of the development of unmanned vehicles for industrial applications are the automation of a truck-loading task using an unmanned excavator [1] and the systematic synthesis for the construction of an autonomous vehicle for a mining task [2]. Particularly, several research results are found in the development of an automatic industrial forklift [3-5,8-10,14-16]. The works presented in [5,14] describe the development of a pallet engagement algorithm by using a vision system, while the work in [15] presents a different approach for

localization and pick-up of the pallet by using a laser scanner. The optimization techniques in using a vision system for the navigation of autonomous forklifts are presented in [4,9,14], while the work in [10] describes the development of a simulator for the optimization of multi-AGV operations in an industrial environment. Another work on the automation of a hot metal carrier, which is a forklift-type vehicle being used to move molten metal in aluminum smelters, is presented in [16]. An extensive description for industrial forklift automation as well as a road-following control algorithm using a camera is presented in [8]. One of the drawbacks of this road-following algorithm is that its performance depends on environment luminance, which can vary greatly in industrial conditions [15].

The problem of path following control for mobile robots and unmanned vehicles has been extensively researched during the last decade. A robust control design for path following of a farm tractor is proposed in [17]. Although the robust control offers a uniform and bounded solution, its control law requires a wide range of control input and fast switching action which can be constrained by the mechanical issues on its practical implementation [20]. On the other hand, a path following control based on the measurement of a real-time kinematic global positioning system (RTK-GPS) is proposed in [18] for guiding a tractor truck. The proposed control method requires accurate estimation of the instantaneous position of the farm truck, therefore a mild error on positioning estimation could lead to a failed control action. A path following control algorithm using the chained form and its application to control a car with  $n$ -trailer is presented in [21]. The proposed control law is derived using a different structure of the chained form called the Skew Symmetric Chained Form, and its objective is only to regulate the lateral error of the car. Latest results on the design of path following control by considering the uncertainties and the slip of the mobile robots are presented in [19,20].

This paper focuses on the development of a feedback path following control for an unmanned autonomous forklift based on its kinematic model. The aim of the

Manuscript received February 9, 2008; revised August 26, 2008 and November 6, 2008; accepted December 15, 2008. Recommended by Editorial Board member Sooyong Lee under the direction of Editor Jae-Bok Song. This work was supported by the Korea Research Foundation Grant funded by the Korean Government (MOEHRD) (The Regional Research Universities Program/ Institute of Logistics Information Technology).

Tua Agustinus Tamba and Keum-Shik Hong are with the School of Mechanical Engineering, Pusan National University, 30 Jangjeon-dong, Gumjeong-gu, Busan 609-735, Korea (e-mails: {tua\_tamba, kshong}@pusan.ac.kr).

Bonghee Hong is with the Department of Computer Science and Engineering, Pusan National University, 30 Jangjeon-dong, Gumjeong-gu, Busan 609-735, Korea (e-mail: dlab@pusan.ac.kr)

\* Corresponding author.

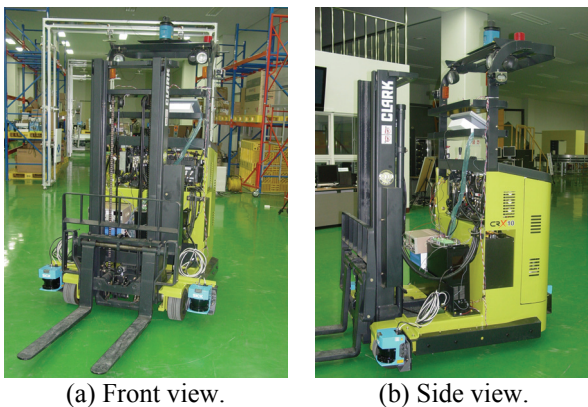
proposed feedback control algorithm is to force the forklift to follow a reference path provided by a path planner. To build such a controller, a representation of the forklift kinematics in terms of the reference path variables is derived. The proposed algorithm can be applied in various environments, since the path following controller does not rely on the environment luminance condition.

The contributions of this paper are the following. A system configuration of the unmanned forklift equipped with sensors and a control PC is described. The kinematics of the forklift with a spin-turn mechanism is then presented. Typical things on this model that makes it different from the general mobile robot or car-like vehicle kinematics [22,23] are the offset  $a$  and three caster wheels (see Fig. 5). A feedback control law for path following of the forklift in terms of path variables is also derived. The proposed control law is derived based on the original structure of the chained form introduced in [12], and the objective in [21] is extended to include the lateral and orientation errors between the actual and desired positions of the unmanned forklift.

This paper is structured as follows. In Section 2, a system configuration for the development of an unmanned autonomous industrial forklift is presented. The kinematics of the forklift in the inertia frame and its representation in path variables are analyzed in Section 3. In Section 4, a feedback control law that makes the radial and orientation errors of the forklift with respect to the reference path equal to zero is derived. In Section 5, simulation and experimental results are presented. Conclusions are given in Section 6.

## 2. SYSTEM CONFIGURATION

The vehicle to be automated in this paper is a standard industrial forklift CRX-10 produced by the CLARK company, see Fig. 1. The forklift body is mounted on four wheels: two caster wheels at the front side and one small caster wheel at the right rear side without any ability of steering or traction, and one main wheel at the left rear side for driving and steering of the forklift, see Fig. 5. The dimension (length x width x height) of the forklift is 2680 x 1170 x 2260mm, and its velocity is



(a) Front view.

(b) Side view.

Fig. 1. Clark CRX-10 forklift equipped with sensors.

limited up to 10 km/h both for empty and loaded operations. To achieve autonomy, the forklift is modified so that all the necessary sensors and a PC for steering and driving motors are attached. The main requirement in automating the forklift is to provide the ability for dual operations, that is, the forklift can be operated in the unmanned mode as well as in the (original) manual mode.

The used sensors are the following. For the purpose of 3-D map building, one LRF NAV 200 (SICK) with 360° scanning ability is attached at the top of the forklift. Three LMS 200-30106 LRFs (SICK) with 180° scanning ability are also attached: two at the front left/right sides and one at the rear side. To detect obstacles in the near left/right sides of the forklift, ten STMA-506MD ultrasonic sensors are attached around the forklift. For detecting moving objects and measuring the pallet position, three HVR-200 cameras are also attached: two cameras at the forklift body (left and right) and one camera at the right fork. The industrial PC is used as a main control unit that collects data from the sensors and performs unmanned autonomous navigations.

As shown in Fig. 2, the motion command for the unmanned forklift is generated based on the information of its pose provided by several sensors. The absolute pose of the forklift in the global reference coordinate is determined on a given map based on the data from ultrasonic satellite and gyro sensor. The present pose and speed of the forklift from its initial point is calculated using the data from wheel encoder and gyro sensor. The information about the forklift environment (obstacles,

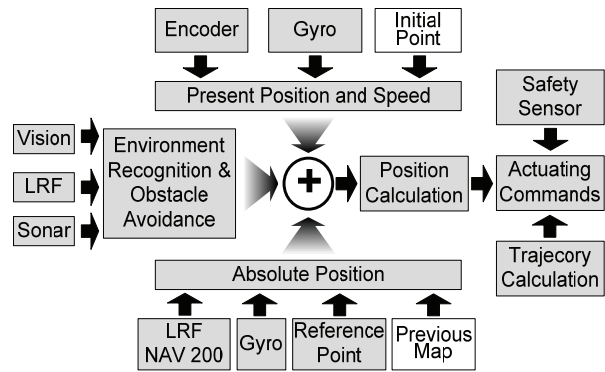


Fig. 2. Sensors for localization, map building, and obstacle avoidance.

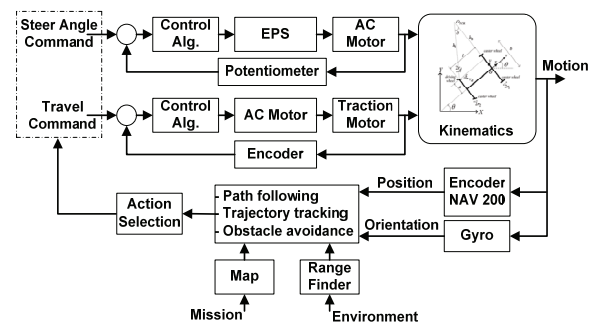


Fig. 3. Steering and traction control for navigation.

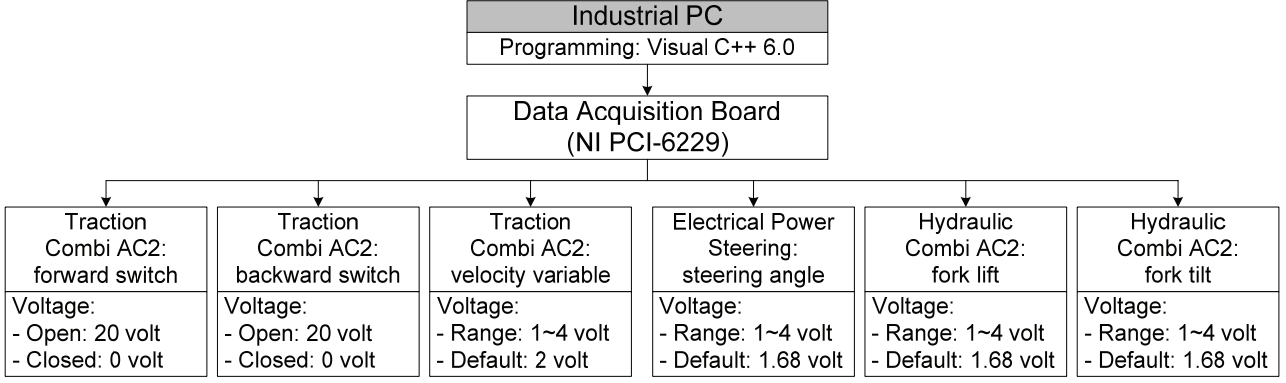


Fig. 4. Signal configuration for a typical industrial forklift.

workspace structure, etc.) is obtained by using vision, laser range finder, and sonar sensors. Based on the current pose, speed, and the information about the change on its working environment, the position of the forklift with respect to its goal point on the reference frame can be calculated. The control command to actuate the motion of the forklift is then generated by considering the trajectory to the goal pose and the safety of its motions.

The control inputs for the forklift consist of linear and angular velocities. Fig. 3 show the navigation schematic of the forklift. The appropriate control signal is determined by an action selection algorithm based on the tasks (following a path, tracking a trajectory, avoiding obstacles, etc.) that needs to be accomplished by the autonomous forklift. Fig. 4 shows the signal configuration for the implementation of the steering and traction control on the forklift.

### 3. FORKLIFT KINEMATICS

#### 3.1. Kinematics in the inertial frame

In Fig. 5, let  $O-X-Y$  and  $o-x-y$  be the inertia frame and the body coordinate frame attached to the forklift, respectively. Let  $v$  and  $\theta$  be the velocity of the forklift in the  $x$ -direction and the rotational angle of the  $x$ -axis with respect to the  $X$ -axis. Let  $\delta$  be the steering angle of the driving wheel. Under the assumption that the wheels do not slip, let  $O_{ICR}$  be the instantaneous center of rotation of the forklift. Finally, let  $l$  and  $a$  be the length of the forklift and the offset of the center of the driving wheel from the centerline of the body, respectively.

Using the geometry in Fig. 5, the distance between  $O_{ICR}$  to the center of the driving wheel becomes

$$h_1 = \frac{l}{\sin \delta}. \quad (1)$$

Then the following relationship can be derived.

$$\dot{\theta} = \frac{v_d}{h_1} = \frac{v}{h_1 \cos \delta + a}, \quad (2)$$

where  $v_d$  is the velocity of the driving wheel characterized by the following relationship

$$v_d = r_d \omega_d, \quad (3)$$

where  $r_d$  is the radius of the driving wheel, and  $\omega_d$  is the angular velocity of the driving wheel, respectively. Therefore, the linear velocity of the forklift becomes

$$v = r_d \omega_d \left( \cos \delta + \frac{a \sin \delta}{l} \right). \quad (4)$$

Finally, the kinematics relationship between two input variables  $\{v_d, \dot{\delta}\}$ , where  $\dot{\delta}$  is the rate of change of the steering angle, and four generalized variables  $\{X, Y, \theta, \delta\}$  (or two output variables  $\{v, \dot{\theta}\}$ ) is given as follows.

$$\dot{X} = v \cos \theta = r_d \omega_d \left( \cos \delta + \frac{a \sin \delta}{l} \right) \cos \theta,$$

$$\dot{Y} = v \sin \theta = r_d \omega_d \left( \cos \delta + \frac{a \sin \delta}{l} \right) \sin \theta,$$

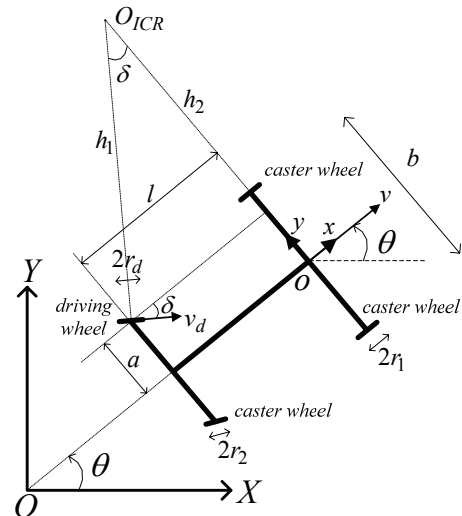


Fig. 5. Schematic of the forklift with a spin-turn steering mechanism.

$$\begin{aligned}\dot{\theta} &= \frac{r_d \omega_d \sin \delta}{l}, \\ \dot{\delta} &= \omega_s.\end{aligned}\quad (5)$$

### 3.2. Kinematics in the path coordinates

This section describes a different mathematical model of the forklift kinematics. This new model relates the desired path coordinates with the input variables. Fig. 6 shows the position and orientation errors between the actual position and the desired path to be followed by the forklift.

Let  $\varphi(x_t, y_t)$  be a curve of the desired path to be followed by the forklift, and the distance along the path is parameterized with  $s(t)$ . The following relationship can be obtained for  $s(t)$ .

$$s(t) = \int_0^t v_t(\tau) d\tau + s(0), \quad (6)$$

where  $s(0)$  is the initial distance along the path, and

$$v_t(t) = \sqrt{\dot{x}_t^2(t) + \dot{y}_t^2(t)} \quad (7)$$

is the linear speed of a projected point  $o_{proj}$  of the origin of the body coordinate,  $o$ , on the path  $s$ . Let  $d$  denote the lateral distance between the forklift reference point,  $o$ , and the reference path to be followed. Let the positive sign of  $d$  represent the condition that the position of the reference path is on the right-hand side of the forklift and the negative sign of  $d$  represent the condition that the position of the reference path is on the left-hand side of the forklift. Let  $\theta_e$  denote the orientation error of the forklift with respect to the reference path, which can be defined as follows.

$$\theta_e = \theta - \theta_t, \quad (8)$$

where  $\theta_t$  denotes the desired orientation of the forklift, which is tangent to the desired path,  $s$ . Based on Fig. 6, the curvature  $\kappa(s)$  for any given point on the reference path at each instant of time can be drawn as follows [7].

$$\begin{aligned}\kappa(s) &= \lim_{\Delta s \rightarrow 0} \frac{\Delta \theta_t}{\Delta s} = \frac{d\theta_t}{ds} \\ &= \frac{d\theta_t}{dt} \cdot \frac{dt}{ds} = \frac{\dot{\theta}_t(t)}{\dot{s}(t)}.\end{aligned}\quad (9)$$

The representation of the reference path in path variables  $\{s, d, \theta_e, \delta\}$  can be derived as follows.

$$\begin{aligned}\dot{s} &= \frac{v \cos \theta_e}{(1-d(t)\kappa(s))}, \\ \dot{d} &= v \sin \theta_e, \\ \dot{\theta}_e &= \dot{\theta}(t) - \dot{\theta}_t(t) = \dot{\theta}(t) - \kappa(s)\dot{s}(t), \\ \dot{\delta} &= \omega_s.\end{aligned}\quad (10)$$

The substitution of (4) into (10) results in the following

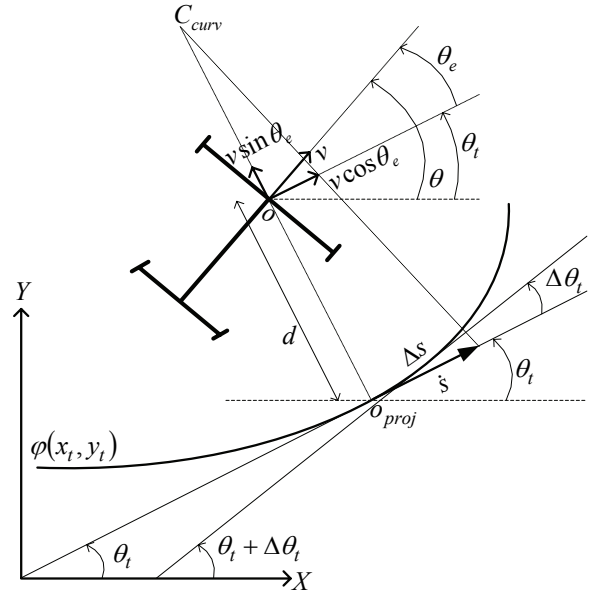


Fig. 6. Kinematic model of the forklift in the path variables.

equations.

$$\begin{aligned}\dot{s}(t) &= \frac{v_d \cos \theta_e \left( \cos \delta + \frac{a \sin \delta}{l} \right)}{(1-d(t)\kappa(s))}, \\ \dot{d}(t) &= v_d \sin \theta_e(t) \left( \cos \delta + \frac{a \sin \delta}{l} \right), \\ \dot{\theta}_e(t) &= \frac{v_d \sin \delta}{l} - \frac{v_d \kappa(s) \cos \theta_e \left( \cos \delta + \frac{a \sin \delta}{l} \right)}{(1-d(t)\kappa(s))}, \\ \dot{\delta}(t) &= \omega_s.\end{aligned}\quad (11)$$

Since the inputs to the forklift system are  $v_d$  and  $\omega_s$ , (11) can be rewritten in the following compact form.

$$\begin{aligned}\begin{bmatrix} \dot{s} \\ \dot{d} \\ \dot{\theta}_e \\ \dot{\delta} \end{bmatrix} &= \begin{bmatrix} \frac{\cos \theta_e \left( \cos \delta + \frac{a \sin \delta}{l} \right)}{(1-d(t)\kappa(s))} \\ \sin \theta_e \left( \cos \delta + \frac{a \sin \delta}{l} \right) \\ \frac{\sin \delta}{l} - \frac{\kappa(s) \cos \theta_e \left( \cos \delta + \frac{a \sin \delta}{l} \right)}{(1-d(t)\kappa(s))} \\ 0 \end{bmatrix} v_d \\ &+ \begin{bmatrix} 0 \\ 0 \\ 0 \\ 1 \end{bmatrix} \omega_s,\end{aligned}\quad (12)$$

where  $v_d$  and  $\omega_s$  denote the linear and steering angular velocities of the forklift driving wheel,

respectively. (12) is a nonlinear system with four state variables  $(s, d, \theta_e, \delta)$  and two input variables  $(v_d$  and  $\omega_s)$ .

#### 4. CONTROL LAW DESIGN

Fig. 7(a) shows a block diagram of the proposed feedback controller for position control and Fig. 7(b) depicts a navigation architecture for unmanned operation of the forklift. The control objective in this paper is to design a controller that will make the lateral error  $d$  and orientation error  $\theta_e$  in (12) equal to zero, so that the forklift can follow the desired trajectory. To design such a controller, a new coordinate transformation called the chained form, which was introduced in [3], is applied to (12).

##### 4.1. Coordinate transformation in chained form

The chained form is one of the canonical structures for the kinematic modeling of a nonholonomic system. This form is very useful because it provides a very controllable structure of a system in the systematic development of a control strategy.

A system with 2 inputs and  $n$  state variables can be written as a  $(2, n)$  chained form as follows [12].

$$\begin{aligned} \dot{x}_1 &= u_1, \\ \dot{x}_2 &= u_2, \\ \dot{x}_3 &= x_2 u_1, \\ &\vdots \\ \dot{x}_n &= x_{n-1} u_1. \end{aligned} \quad (13)$$

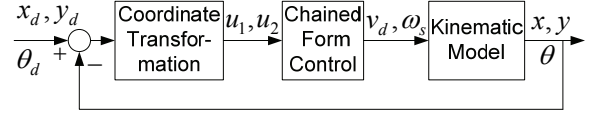
Based on the path coordinate model derived in the previous section, the forklift studied in this paper has four state variables. Therefore, the forklift path coordinate (12) can be described in the following (2,4) chained form.

$$\begin{aligned} \dot{x}_1 &= u_1, \\ \dot{x}_2 &= u_2, \\ \dot{x}_3 &= x_2 u_1, \\ \dot{x}_4 &= x_3 u_1. \end{aligned} \quad (14)$$

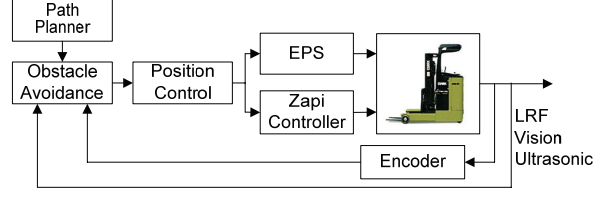
The coordinate transformation for the state variables is defined as

$$\begin{aligned} x_1 &= s, \\ x_2 &= -\kappa'(s)d(t) \tan \theta_e - \frac{\kappa(s)(1-d(t)\kappa(s))(1+\sin^2 \theta_e)}{\cos^2 \theta_e} \\ &\quad + \frac{\sin \delta (1-d(t)\kappa(s))^2}{\cos^3 \theta_e (l \cos \delta + a \sin \delta)}, \\ x_3 &= \tan \theta_e (1-d(t)\kappa(s)), \\ x_4 &= d, \end{aligned} \quad (15)$$

where  $\kappa'(s)$  is the derivative of the path curvature



(a) Control block diagram.



(b) Navigation architecture.

Fig. 7. Navigation architecture and control block diagram.

$\kappa(s)$  with respect to  $s$ . The inputs transformation are defined as

$$\begin{aligned} u_1 &= \frac{\cos \theta_e \left( \cos \delta + \frac{a \sin \delta}{l} \right)}{1-d(t)\kappa(s)} v_d, \\ u_2 &= \alpha_2(q)\omega_s + \alpha_1(q)u_1, \end{aligned} \quad (16)$$

where

$$\begin{aligned} \alpha_1(q) &= \frac{\partial x_2}{\partial s} + \frac{\partial x_2}{\partial d} (1-d(t)\kappa(s)) \tan \theta_e \\ &\quad + \frac{\partial x_2}{\partial \theta_e} \left[ \frac{\sin \delta (1-d(t)\kappa(s))}{\cos \theta_e (l \cos \delta + a \sin \delta)} - \kappa(s) \right], \\ \alpha_2(q) &= \frac{l(1-d(t)\kappa(s))^2}{\cos^3 \theta_e (l \cos \delta + a \sin \delta)^2}. \end{aligned} \quad (17)$$

##### 4.2. A time varying feedback control law

The control design via a smooth time varying feedback presented in this paper is based on the work presented in [11,13]. This paper presents a modification of their work for the development of a path following control by using the chained form of the path coordinate model (12). Since the objective of the control design is to make the lateral error  $d$  and orientation error  $\theta_e$  in (12) equal to zero, the purpose of the designed path following control is to make  $x_2$  and  $x_4$  in (14) equal to zero.

For a system given in the chained form, its variables can be rearranged as

$$\eta = (\eta_1, \eta_2, \dots, \eta_{n-1}, \eta_n) = (x_1, x_n, \dots, x_3, x_2). \quad (18)$$

Rearranging (14) in the structure of (18), the following new chained form can be obtained.

$$\dot{\eta} = h_1(\eta)u_1 + h_2(\eta)u_2, \quad (19)$$

where

$$h_1(\eta) = [1 \quad \eta_3 \quad \dots \quad \eta_n \quad 0]^T,$$

$$h_2(\eta) = [0 \ 0 \ \dots \ 0 \ 1]^T.$$

For the forklift kinematics, the above reordering is an exchange between the second and fourth coordinates. Let  $\eta = (\eta_1, \eta^*)$ , where  $\eta^* = (\eta_2, \eta_3, \dots, \eta_n)$ , the chained form (19) can be rewritten as follows.

$$\begin{aligned} \dot{\tilde{\eta}}_1 &= 0, \\ \dot{\eta}^* &= \begin{bmatrix} \dot{\eta}_2 \\ \dot{\eta}_3 \\ \dot{\eta}_4 \end{bmatrix} = \begin{bmatrix} 0 & u_1(t) & 0 \\ 0 & 0 & u_1(t) \\ 0 & 0 & 0 \end{bmatrix} \eta^* + \begin{bmatrix} 0 \\ 0 \\ 1 \end{bmatrix} u_2, \end{aligned} \quad (20)$$

where

$$\tilde{\eta}_1 = \eta_1 - \int_0^t u_1(\tau) d\tau.$$

The structure  $\eta^*$  in (20) is similar to the controllable canonical form of linear system. If  $u_1$  is priori assigned as a constant and nonzero, the second part in (20) is clearly controllable. With this priori knowledge,  $x_1$  varies monotonically with time and the differentiation with respect to time can be replaced by differentiation with respect to  $\eta_1$  as shown below.

$$\begin{aligned} \frac{d}{dt} &= \frac{d}{d\eta_1} \dot{\eta}_1 = \frac{d}{d\eta_1} u_1, \\ &= \text{sign}(u_1) |u_1| \frac{d}{d\eta_1}. \end{aligned} \quad (21)$$

The above procedure is known as the input scaling procedure [11]. With the change of variable  $u_1$ , the variables  $\dot{\eta}_2, \dot{\eta}_3$ , and  $\dot{\eta}_4$  in (20) can be rewritten as

$$\begin{aligned} \eta_2^{[1]} &= \text{sign}(u_1) \eta_3, \\ \eta_3^{[1]} &= \text{sign}(u_1) \eta_4, \\ \eta_4^{[1]} &= \text{sign}(u_1) u_2', \end{aligned} \quad (22)$$

where

$$\eta_i^{[j]} = \text{sign}(u_1) \frac{d^j \eta_i}{d\eta_1^j} \quad \text{and} \quad u_2' = \frac{u_2}{u_1}.$$

The relationship in (22) is a controllable linear time-invariant system that admits an exponentially stable linear feedback in the following form [6].

$$u_2'(\eta_2) = -\text{sign}(u_1)^{(n-1)} \sum_{i=1}^{n-1} k_i \eta_2^{[i-1]}. \quad (23)$$

Hence the time-varying control can be calculated as

$$u_2(\eta_2, t) = u_1(t) u_2'(\eta_2). \quad (24)$$

For the chained form of the forklift in (22), the stable and controllable linear feedback form is given by

$$u_2'(\eta_2, \eta_3, \eta_4) = -\text{sign}(u_1) (k_1 \eta_2 + k_2 \text{sign}(u_1) \eta_3 + k_3 \eta_4), \quad (25)$$

and the path following feedback control law becomes

$$u_2(\eta_2, \eta_3, \eta_4, t) = -k_1 |u_1(t)| \eta_2 - k_2 u_1(t) \eta_3 - k_3 |u_1(t)| \eta_4. \quad (26)$$

Finally, in rewriting the inputs of the chained form by using the measured variables and errors, the linear and angular velocities in (16) become

$$v_d = \frac{(1-d(t)\kappa(s)) u_1}{\cos \theta_e \left( \cos \delta + \frac{a \sin \delta}{l} \right)}, \quad (27)$$

$$\omega_s = \frac{1}{\alpha_2(q)} \left( -k_1 |u_1(t)| \eta_2 - k_2 u_1(t) \eta_3 - k_3 |u_1(t)| \eta_4 - \alpha_1(q) u_1 \right), \quad (28)$$

where  $(\alpha_1, \alpha_2)$  and  $(\eta_2, \eta_3, \eta_4)$  are defined in (17) and (18), respectively.

## 5. SIMULATIONS AND EXPERIMENTS

First, simulation results of the control algorithm derived in Section 3 for the path following control of the forklift is discussed. The reference path is assumed to be a circle of radius 5 meters. With this circular path, the curvature is 1/5. Since the curvature is constant, its time derivative is equal to zero.

The initial position of the forklift is set to  $(x, y, \theta) = (0, 2.25, 135^\circ)$ , which gives the initial lateral error,  $d$ , of 0.25 meters and initial orientation error,  $\theta_e$ , of  $45^\circ$ . The linear velocity of the forklift is set to 1 m/s, and the gains for the feedback controller are set to  $(k_1, k_2, k_3) = (10, 10, 10)$ .

Fig. 8 shows the simulation result for the circular path, in which  $u_1$  and  $u_2$  in Fig. 9 are the control inputs in chained form. The lateral error  $d$  and orientation error  $\theta_e$  in Figs. 10 and 11 show that the proposed feedback controller makes the radial and orientation errors go to zero, thus forces the forklift to follow the predetermined path. The actual linear velocity  $v_d$  and angular velocity  $\omega_s$  are depicted in Figs. 12 and 13, respectively.

The proposed path following control algorithm was also verified by experiments. The conducted experiments are to show the unmanned forklift to follow a reference path with via points (VPs). The initial and goal points,  $(x_0, y_0)$  and  $(x_f, y_f)$ , are set to (7300, 6150) and (2500, 1080)mm, respectively. The first reference path is a sequence of three straight lines that connect three VPs in  $(x, y)$  coordinates as follows: VP1 (5300, 5300), VP2 (3700, 5300), and VP3 (3700, 2500), respectively. Fig. 14 shows the experimental result, whereas Figs. 15

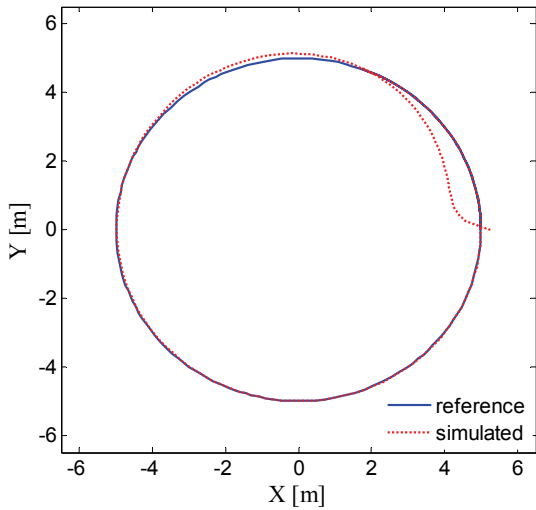


Fig. 8. Simulation for a circular desired trajectory.

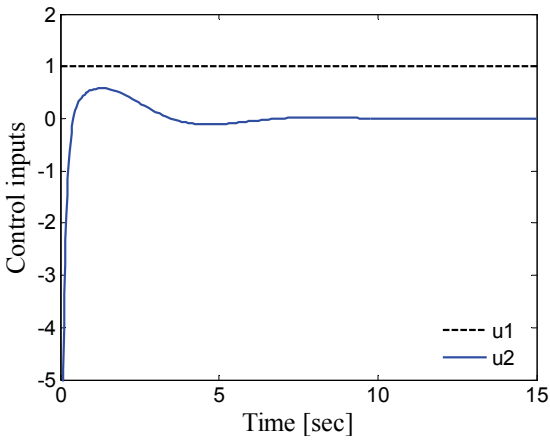


Fig. 9. Control inputs,  $u_1$  and  $u_2$ , of (26).

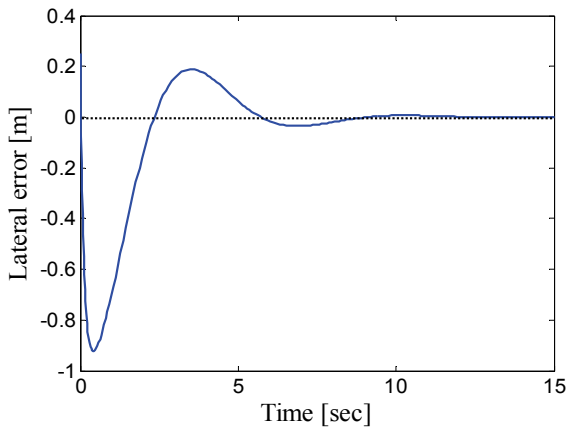


Fig. 10. Lateral error between the forklift and the desired path.

and 16 show the linear and angular velocities in obtaining Fig. 14, respectively. It is seen that the proposed path following control algorithm can make the unmanned forklift follow the given reference path.

The reference trajectory for a second experiment is shown in Fig. 17, which consists of four straight lines and four arcs. The length of each straight line is 2 meters,

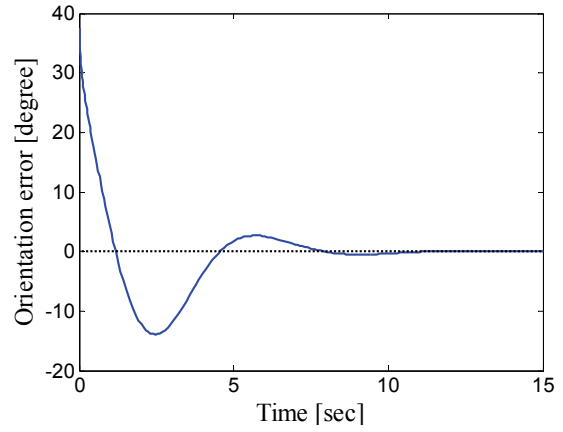


Fig. 11. Orientation error between the forklift and the desired path.

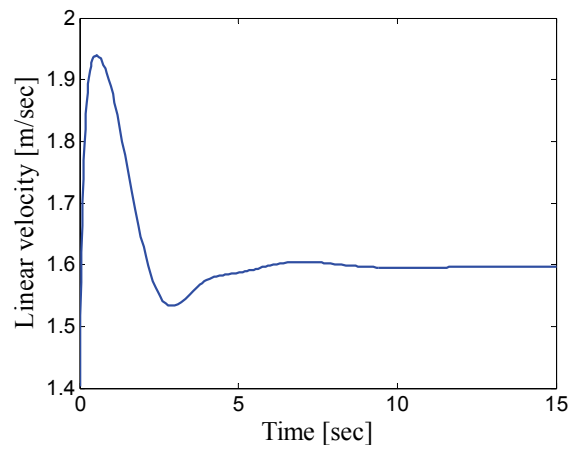


Fig. 12. Linear velocity  $v_d$  of the steering wheel.

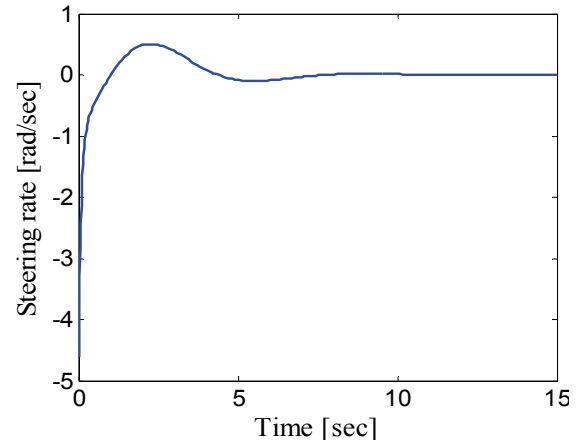


Fig. 13. Angular velocity  $\omega_s$  of the steering wheel.

whereas the radius of each arc segment is 1 meter. The initial and goal points are the same, that is, (5500, 5500). The experimental result shows that there exist some errors between the actual and the reference paths, particularly when going around four corner points. But, the overall performance is acceptable. Figs. 18 and 19 show the corresponding linear and angular velocities, respectively.

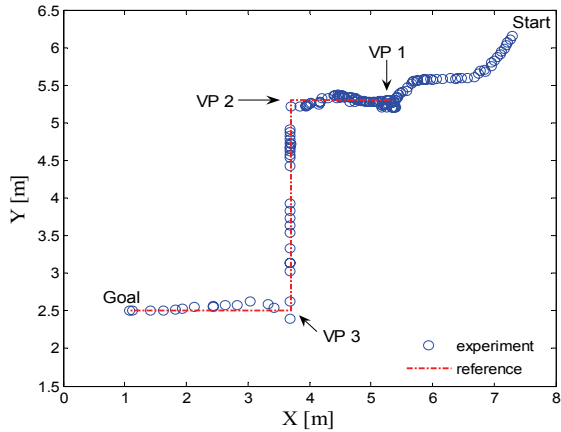


Fig. 14. Experimental result when the reference path involves only straight lines.

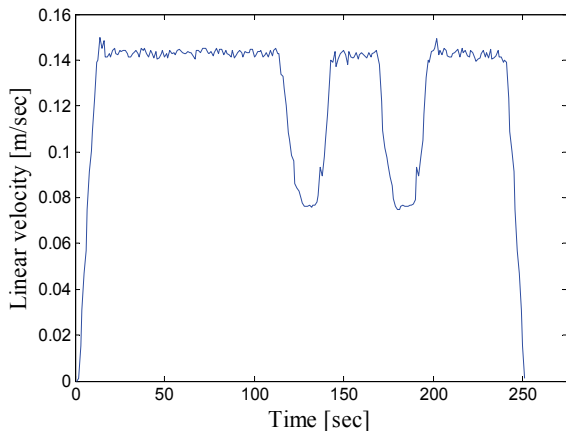


Fig. 15. Linear velocity  $v_d$  for Fig. 14.

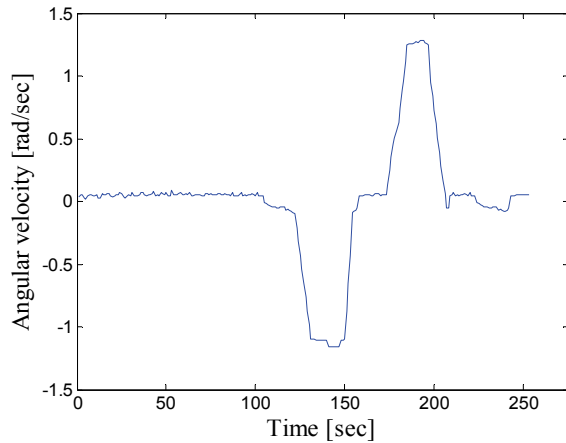


Fig. 16. Angular velocity  $\omega_s$  for Fig. 14.

**6. CONCLUSIONS**

In this paper, a system configuration using laser and vision sensors and a PC controller for the development of an unmanned autonomous forklift was presented. A kinematic model of the spin-turn mechanism forklift was derived. The obtained kinematic equations were transformed to the equations represented by path variables.

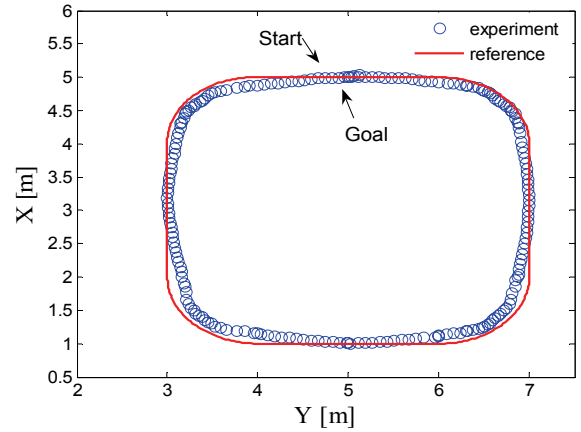


Fig. 17. Experimental result when the reference path includes both straight lines and arcs.

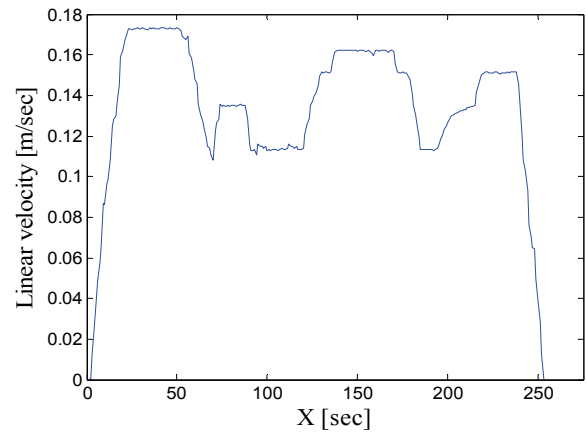


Fig. 18. Linear velocity  $v_d$  for Fig. 17.

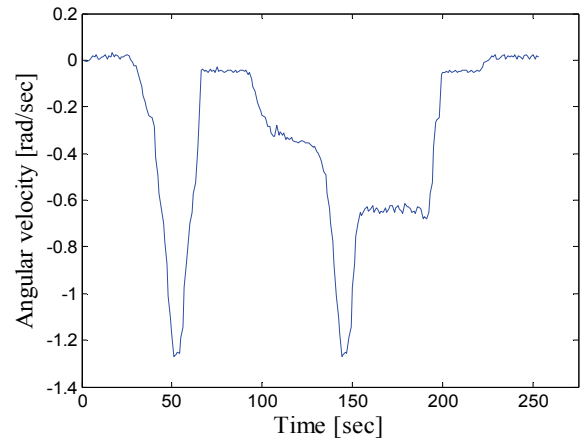


Fig. 19. Angular velocity  $\omega_s$  for Fig. 17.

For following a desired path, a time varying feedback control law via the chained form was derived. The simulation and experiment results showed that the proposed path-following control algorithm gives a good performance in dealing with a reference path with constant curvatures. However, it was seen that the performance decreases when the curvature of the reference path changes severely. Developing an estimation algo-



rithm of the reference path curvature is left as a future work.

#### REFERENCES

- [1] A. Stenz, J. Bares, S. Singh, and P. Rowe, "A robotic excavator for autonomous truck loading," *Proc. of the IEEE/RSJ Int. Conf. on Intelligent Robots and Systems*, vol. 3, pp. 1885-1893, October 1998.
- [2] J. Gutiérrez, J. L. Gordillo, and I. López, "Configuration and construction of an autonomous vehicle for a mining task," *Proc. of IEEE Int. Conf. on Robotics and Automation*, pp. 2010-2016, April 2004.
- [3] H. Frohn and W. V. von Seelen, "VISOCAR: An autonomous industrial transport vehicle guided by visual navigation," *Proc. of IEEE Int. Conf. on Robotics and Automation*, vol. 2, pp. 1155-1159, May 1989.
- [4] R. K. Miller, D. G. Stewart, W. H. Brockman, and S. B. Skaar, "A camera space control system for an automated forklift," *IEEE Trans. on Robotics and Automation*, vol. 10, no. 5, pp. 710-716, October 1994.
- [5] G. Garibotto, S. Masciangelo, M. Ilic, and P. Bassino, "ROBOLIFT: A vision guided autonomous fork-lift for pallet handling," *Proc. of IEEE/RSJ Int. Conf. on Robots and Systems*, pp. 656-663, November 1996.
- [6] J. P. Laumond, *Robot Motion Planning and Control*, Springer-Verlag, Toulouse, 1998.
- [7] D. John and R. D. Nelson, "Dictionary of Mathematics," pp. 81-82, Penguin Books, England, 1989.
- [8] F. J. Rodríguez, M. Mazo, and M. A. Sotelo, "Automation of an industrial forklift truck, guided by artificial vision in open environment," *Autonomous Robot*, vol. 5, no. 2, pp. 215-231, May 1998.
- [9] J. Pagès, X. Armangué, J. Salvi, J. Freixenet, and J. Martí, "A computer vision system for autonomous forklift vehicles in industrial environments," *Proc. of the 9th Mediterranean Conf. on Control and Automation*, June 2001.
- [10] K. Petrinc, Z. Kovačić, and A. Marozin, "Simulator of multi-AGV robotic industrial environments," *Proc. of IEEE Int. Conf. on Industrial Technology*, vol. 2, pp. 979-983, December 2003.
- [11] C. A. Samson, A. De Luca, and G. Oriolo, *Feedback Control of a Nonholonomic Car-like Robot*, Dipartimento di Informatica e Sistemistica, Università di Roma "La Sapienza," 2004.
- [12] R. M. Murray and S. S. Sastry, "Nonholonomic motion planning: Steering using sinusoids," *IEEE Trans. on Automatic Control*, vol. 38, no. 5, pp. 700-716, May 1993.
- [13] I. Schworer, *Navigation and Control of Autonomous Vehicle*, M.S. Thesis, Virginia Polytechnic Institute and State University, 2005.
- [14] M. Seelinger and J. D. Yoder, "Automatic visual guidance of a forklift engaging a pallet," *Robotics and Autonomous Systems*, vol. 54, no. 12, pp. 1026-1038, August 2006.
- [15] D. O. Lecking, O. Wulf, and B. Wagner, "Variable pallet pick-up for automatic guided vehicles in industrial environments," *Proc. of IEEE Int. Conf. on Emerging Technologies and Factory Automation*, pp. 1169-1174, September 2006.
- [16] J. Roberts, A. Tews, C. Pradalier, and K. Usher, "Autonomous hot metal carrier-navigation and manipulation with a 20 ton industrial vehicle," *Proc. of IEEE Int. Conf. on Robotics and Automation*, pp. 2770-2771, April 2007.
- [17] H. Fang, R. Lenain, B. Thuilot, and P. Martinet, "Robust adaptive control of automatic guidance of farm vehicles in the presence of skidding," *Proc. of IEEE Int. Conf. on Robotics and Automation*, pp. 3113-3118, April 2005.
- [18] B. Thuilot, C. Cariou, and P. Martinet, "Automatic guidance of a farm tractor along curved paths, using a unique CD-DGPS," *Proc. of IEEE Int. Conf. on Intelligent Robots and Systems*, pp. 674-679, November 2001.
- [19] C. B. Low and D. Wang, "GPS-based path following control for a car-like wheeled mobile robot with skidding and slipping," *IEEE Trans. on Control Systems Technology*, vol. 16, no. 2, pp. 340-347, March 2008.
- [20] P. Coelho and U. Nunes, "Path-following control of mobile robots in presence of uncertainties," *IEEE Trans. on Robotics*, vol. 21, no. 2, pp. 252-261, April 2005.
- [21] C. Samson, "Control of chained systems: Application to path following and time-varying point stabilization," *IEEE Trans. on Automatic Control*, vol. 40, no. 1, pp. 64-77, January 1995.
- [22] G. Kaloutsakis, N. Tsourveloudis, and P. Spanoudakis, "Design and development of an Automated Guided Vehicle," *Proc. of IEEE Int. Conf. on Industrial Technology*, vol. 2, pp. 990-993, December 2003.
- [23] N. M. Dung, V. H. Duy, N. T. Phuong, S. B. Kim, and M. S. Oh, "Two-wheeled welding mobile robot for tracking a smooth curved welding path using adaptive sliding-mode control technique," *International Journal of Control, Automation, and Systems*, vol. 5, no. 3, pp. 283-294, June 2007.



**Tua Agustinus Tamba** received the B.S. degree in Engineering Physics from Institute of Technology Bandung, Indonesia, in 2006. He is currently a graduate student at the School of Mechanical Engineering, Pusan National University, Busan, Korea. His research interests include control of unmanned vehicles and path planning technologies for auton-

omous robots.



**Bonghee Hong** received the B.S., M.S., and Ph.D. degrees in Computer Science and Engineering from Seoul National University in 1982, 1984, and 1988, respectively. Dr. Hong joined the Department of Computer Science and Engineering at Pusan National University (PNU) in 1989 and now he is a Professor. Dr. Hong is the Director of the Research

Institute of Logistics Information Technology (LIT) at PNU. Dr. Hong received the Korean Minister Award in 2006 and the University Excellence Innovation Award in 2007. His current research interests include theory of database systems, RTLS systems, RFID middleware, RFID database, and stream data processing.



**Keum-Shik Hong** received the B.S. degree in Mechanical Design and Production Engineering from Seoul National University in 1979, the M.S. degree in Mechanical Engineering from Columbia University, New York, in 1987, and both the M.S. degree in Applied Mathematics and the Ph.D. degree in Mechanical Engineering from the University of

Illinois at Urbana-Champaign (UIUC) in 1991. From 1991 to 1992, he was a Postdoctoral Fellow at UIUC. Since Dr. Hong joined the School of Mechanical Engineering at Pusan National University, Korea, in 1993, he is now a Professor. During 1982-85, he was with Daewoo Heavy Industries, Incheon, Korea, where he worked on vibration, noise, and emission problems of vehicles and engines. Dr. Hong serves as Editor-in-Chief of the *Journal of Mechanical Science and Technology* and serves as an Associate Editor in various IEEE and IFAC conferences editorial boards. He also served as an Associate Editor for the *Journal of Control, Automation, and Systems Engineering* and has been serving as an Associate Editor for *Automatica* (2000-2006) and as an Editor for the *International Journal of Control, Automation, and Systems* (2003-2005). His laboratory, Integrated Dynamics and Control Engineering Laboratory, was designated as a National Research Laboratory by the Ministry of Science and Technology of Korea in 2003. Dr. Hong received Fumio Harashima Mechatronics Award in 2003 and the Korean Government Presidential Award in 2007. He is a Member of ASME, IEEE, ICROS, KSME, KSPE, KIEE, and KINPR. Dr. Hong's current research interests include nonlinear systems theory, adaptive control, distributed parameter system control, robotics, vehicle control, and innovative control applications to engineering problems.